

Astrophysical S factor for the ${}^7\text{Li}(d, n_0){}^8\text{Be}$ and ${}^7\text{Li}(d, n_1){}^8\text{Be}$ reactions

A. Sabourov, M. W. Ahmed, M. A. Blackston, A. S. Crowell, C. R. Howell, B. A. Perdue, K. Sabourov, A. Tonchev, and H. R. Weller

*Department of Physics, Duke University, Durham, North Carolina 27708, USA, and
Triangle Universities Nuclear Laboratory, Durham, North Carolina 27708, USA*

R. M. Prior and M. C. Spraker

*North Georgia College and State University, Dahlonega, Georgia 30597, USA, and
Triangle Universities Nuclear Laboratory, Durham, North Carolina 27708, USA*

(Received 11 October 2005; published 18 January 2006)

The absolute astrophysical S factor and cross section for the ${}^7\text{Li}(d, n_0){}^8\text{Be}$ and ${}^7\text{Li}(d, n_1){}^8\text{Be}$ reactions have been determined using deuteron beams with energies between 45 and 80 keV. The slope of the S factor is consistent with zero in the n_0 case but is slightly negative in the n_1 case. The S factor for the sum of both neutron groups at c.m. energies below 70 keV is $S(E) = 5400(\pm 1500) - 37(\pm 21)E$ keV b, where E is the c.m. energy in keV.

DOI: [10.1103/PhysRevC.73.015801](https://doi.org/10.1103/PhysRevC.73.015801)

PACS number(s): 27.20.+n

I. INTRODUCTION

The primordial abundance of ${}^7\text{Li}$ is one of the more important diagnostics of the degree of baryon inhomogeneity in early universe models [1]. The ${}^7\text{Li}$ yield is determined from a balance between production and destruction reactions. An accurate knowledge of both types of reactions is necessary for cosmological model calculations to be reliable.

For one set of destruction reactions, the ${}^7\text{Li} + d$ reactions, recent primordial nucleosynthesis codes have incorporated resonant terms in addition to the direct term [1]. These reaction rates were calculated using measured astrophysical S factors. However, the direct term for energies below the 280-keV resonance was assumed to have zero slope on the basis of (d, n) and (d, p) data taken between 1.6 and 2.0 MeV [1,2].

The cross section for the (d, n) channel, which is dominant over the (d, p) channel, has been studied below a c.m. energy of 280 keV [3,4] and has been measured at c.m. energies down to 50 keV [3]. The S factor was experimentally determined at effective c.m. energies of 50, 83.5, and 100 keV [3], which indicated that the slope of the S factor is nonzero and negative.

The present measurements were undertaken to determine the slope and absolute value of the S factor and the absolute cross section for the ${}^7\text{Li}(d, n){}^8\text{Be}$ reaction at c.m. energies below 70 keV for the n_0 transition to the 0^+ ground state of ${}^8\text{Be}$ and for the n_1 transition to the 2^+ first excited state. An investigation into the n_2 transition to the 4^+ second excited state was also undertaken, but the spectrum in this region was too complicated to extract reliable results. The present results indicate that the S factor for the n_0 transition has a slope consistent with zero, whereas the S factor for the n_1 transition has a small negative slope at c.m. energies below 70 keV. These results are in reasonable agreement with the zero-slope S -factor assumption of Ref. [1].

II. EXPERIMENTAL METHOD

The Triangle Universities Nuclear Laboratory (TUNL) atomic beam polarized-ion source produced unpolarized

deuteron beams for measurements at three separate energies: $E_d = 45, 60,$ and 80 keV. Beam currents averaged about $40 \mu\text{A}$. Data sets at 80 and 60 keV were taken at the beginning and end of the week-long run with the 45-keV set taken in the middle.

The target was made *in situ* in the vacuum chamber. Enriched 99% ${}^7\text{Li}$ was evaporated directly onto the 3-mm-thick aluminum target chamber face and was replenished every 4 h. The deposited lithium layer was thick enough to stop the deuteron beam and was previously determined to be Li_2O . The measurements that established this are described in detail in Prior *et al.* [5]. Target conditions were monitored by observing the counting rate as well as visual inspection of the target.

The emitted neutrons were detected using six 12.7-cm-diameter and three 11.4-cm-diameter organic liquid scintillators containing BC-501 fluid. Detectors were placed approximately 43 cm from the target face at angles of $0^\circ, 23^\circ, 45^\circ, 68^\circ, 90^\circ, 113^\circ, 135^\circ,$ and 150° . The detector efficiency is vital to the determination of the total cross section and S factor; this efficiency is well modeled for given fractions of the ${}^{137}\text{Cs}$ edge using the Physikalisch-Technische Bundesanstalt (PTB) group's Monte Carlo programs NRESP7 and NEFF7 [6] and has been experimentally measured previously at TUNL [7,8]. Therefore, the thresholds were carefully set at 1.0 times the ${}^{137}\text{Cs}$ edge (defined to be the point at which the yield falls to one-half its peak value) for these measurements. Data acquisition was configured to utilize pulse-shape discrimination (PSD) to enable separation of the neutrons from the γ -ray background.

Prior to these measurements, the response function for each type of detector was measured using a monoenergetic neutron beam in TUNL's Shielded Source Area (SSA). Fast neutrons were produced via the ${}^2\text{H}(d, n){}^3\text{He}$ reaction. The detector response function was then measured for a neutron energy corresponding to the n_0 group of the ${}^7\text{Li}(d, n){}^8\text{Be}$ reaction ($E_{\text{lab}} = 14$ MeV) and for a neutron energy corresponding to the peak energy of the n_1 group ($E_{\text{lab}} = 11$ MeV). Time-of-flight techniques were used to separate the monoenergetic ${}^2\text{H}(d, n){}^3\text{He}$ neutrons from the lower energy

continuum neutrons generated by breakup reactions. The response functions for the 11- and 14-MeV neutrons had identical shapes, differing only by where the endpoint energy was located. Because the n_1 group has a width of 1.5 MeV, the monoenergetic 11-MeV spectrum was then convoluted with a Breit-Wigner function of the same width to represent the actual response function for that neutron group. To obtain the response function for the n_2 group ($E_{\text{lab}} = 3.4$ MeV), a blank titanium target was implanted with deuterium, and the $E_{\text{lab}} = 2.8$ MeV neutrons from the ${}^2\text{H}(d,n){}^3\text{He}$ reaction were measured at $E_d = 80$ keV. This signal was then convoluted with a Breit-Wigner function of width 3.5 MeV to represent the actual response function for the n_2 group.

In addition to the neutron groups from the ${}^7\text{Li}(d,n){}^8\text{Be}$ reaction, a neutron group from the ${}^2\text{H}(d,n){}^3\text{He}$ reaction was also evident in the spectrum in nearly the same location as the n_2 peak. This state at $E_{\text{lab}} = 2.8$ MeV was fitted with the response function mentioned in the previous paragraph and subtracted from the ${}^7\text{Li}(d,n){}^8\text{Be}$ spectrum. This background peak was identified by studying the rise in its yield in conjunction with the integrated beam current, especially with respect to the time at which a new ${}^7\text{Li}$ target layer was evaporated. Any other room background, γ or neutron, was of sufficiently low energy that it was either eliminated by our threshold setting or low enough in energy to not impact our fitting region.

III. DATA ANALYSIS

The raw neutron spectrum for each angle was fitted with a combination of the measured n_0 , n_1 , n_2 , and ${}^2\text{H}(d,n){}^3\text{He}$ response functions as shown in Fig. 1. To obtain raw n_0 yields, the n_1 , n_2 , and ${}^2\text{H}(d,n){}^3\text{He}$ functions were subtracted from the spectrum; a similar procedure was performed to obtain the n_1 and n_2 yields. For n_0 , the remaining spectrum was summed from approximately 2 to 14 MeV. Because the entire spectral region was not summed, a correction factor was obtained to determine the absolute cross section by dividing the number of counts in the corresponding summation region of the response spectrum by the entire number of counts in the response spectrum. For the n_0 and n_1 states this ratio was generally on the order of 60%. However, for the n_2 state this ratio was 10% on average. More of the spectrum could not be used owing to the efficiency of the detectors changing rapidly below 3 MeV. The small percentage of the spectrum that was usable and disentanglement issues with the neutrons from the ${}^2\text{H}(d,n){}^3\text{He}$ reaction made the n_2 data extraction difficult and unreliable.

Each raw neutron spectrum was also fitted at each angle with just a combination of the measured n_0 and n_1 response functions in the region between approximately 6 and 14 MeV, where the n_2 and ${}^2\text{H}(d,n){}^3\text{He}$ states should have little effect on the data. These yield results agreed with the yield results computed as previously described. For these cases, the ratio of the number of counts in the summed region to those of the entire spectrum was generally 30–50%.

Because the target stops the deuteron beam, the observed yield is the total yield from the beam energy to zero and can

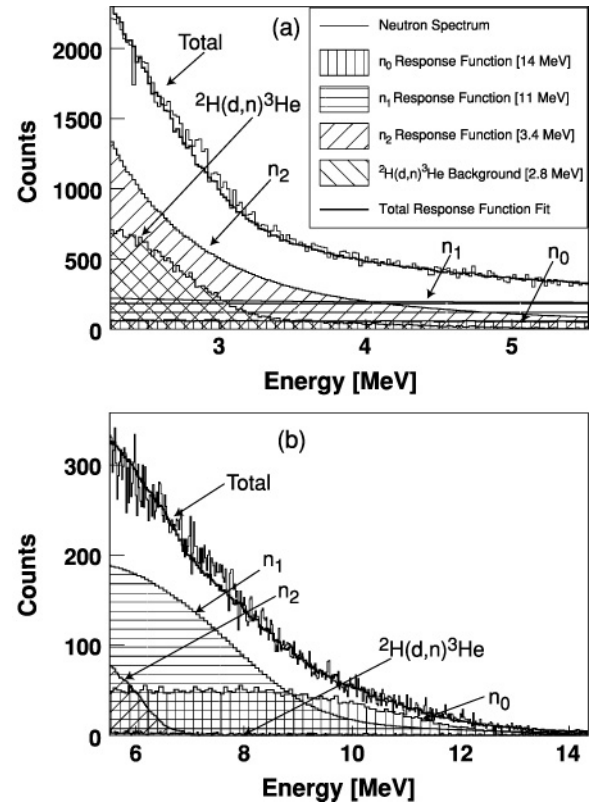


FIG. 1. The measured total neutron spectrum for the ${}^7\text{Li}(d,n){}^8\text{Be}$ reaction at an incident deuteron energy of 80 keV in the fitting region between 2 and 14 MeV. (a) The low-energy end of the fitting region; (b) the high-energy end. The legend in (b) is the same as that in (a). The energy calibration used for the x axis is uncertain to ± 0.5 MeV and was determined by pinpointing the channel corresponding to the 14-MeV endpoint energy of the n_0 state, dividing that channel number by the energy to obtain a calibration factor, and applying that calibration factor to all channels in the spectrum.

be written as

$$Y(E_d) = C \int_{E_d}^0 \frac{\sigma(E)f}{STP(E)} dE, \quad (1)$$

where E_d is the deuteron beam energy, $\sigma(E)$ is the energy-dependent cross section, f is the atomic fraction of the target, and $STP(E)$ is the stopping power of the target for deuterons. The constant C is the total number of incident deuterons times the detector solid angle and efficiency. The raw yield for each angle was normalized by this constant. The cross section can be written in terms of the astrophysical $S(E)$ factor as

$$\sigma(E_{c.m.}) = \frac{S(E_{c.m.})}{E_{c.m.}} e^{-2\pi\eta}, \quad (2)$$

where η is the Sommerfeld parameter and $2\pi\eta = 31.29Z_1Z_2(\mu/E_{c.m.})^{1/2}$. The projectile and target charges are Z_1 and Z_2 , respectively, μ is the reduced mass in amu, and $E_{c.m.}$ is the c.m. energy in keV.

At the low energies of this experiment, the S factor was assumed to be linear with energy:

$$S(E_{c.m.}) = S_0 + S_1 E_{c.m.} \quad (3)$$

TABLE I. Comparison of the yield ratios for a theoretical calculation assuming $S(E)$ is constant and the experimental ratios for the n_0 and n_1 neutron yields. $Y(80)$, $Y(60)$, and $Y(45)$ are the yields at beam energies of 80, 60, and 45 keV, respectively.

	Theoretical constant $S(E)$	Experimental	
		n_0	n_1
$Y(80)/Y(60)$	10	11 ± 1.5	8.4 ± 0.91
$Y(60)/Y(45)$	15	14 ± 3.9	15 ± 2.6

The yield in Eq. (1) can then be calculated for a given beam energy from the values of S_0 and S_1 .

As a preliminary evaluation of our data, the ratios of the experimental yields at each energy were compared to the ratios predicted given a constant S factor, that is, $S_1 = 0$ in Eq. (3). This comparison is shown in Table I and indicates that the slope of the S factor is zero for the n_0 case but not for the n_1 case.

To determine the slope, the integral in Eq. (1) was evaluated numerically, and the slope was determined by fitting the three yields simultaneously. The target was divided into $1 \mu\text{g}/\text{cm}^2$ layers corresponding to less than 1-keV energy loss in the target material. The stopping power of the target was calculated using Anderson and Ziegler's energy-loss equations [9]. By using Eq. (3) as the form of $S(E)$ and starting with arbitrary values for S_0 and S_1 , the yield and energy loss for the first layer was calculated. The yield calculation was then repeated for the next layer at the decreased energy. This process was repeated until the yield of a subsequent layer was less than 0.1% of the yield in the first layer. The sum of the yields from all layers of the target equaled the total yield at the beam energy. This process was performed at all three beam energies and repeated iteratively, by continuously adjusting the values of S_0 and S_1 until the best fit to the measured yields was obtained. The errors in S_0 and S_1 arise from both the statistical uncertainties associated with the experimental yields and the systematic errors from the response function fits to the spectra, from the S -factor fits to the three yields, and from the parameters necessary to determine the absolute scale. The statistical errors were at most 15%; the components of the systematic error, which were added in quadrature, averaged 20% for the response function fits to the spectra and 4% for the parameters that comprised the absolute scale. The errors in the S -factor fits to the three yields, which were also included in the systematic error, were 5% for the S_0 parameter for the n_0 data, 20% for the S_0 parameter for the n_1 data, and 50% for the S_1 parameter for the n_1 data.

The constant C in Eq. (1) allows an absolute scale to be included in the yield calculation and thus in the S -factor and cross-section determination. This scale factor was folded into the S -factor result, giving it units of keV b. Using the results of the S factor derived from the yields, the absolute cross section for each energy was then determined.

IV. EXPERIMENTAL RESULTS AND DISCUSSION

The measured yields as a function of beam energy for the ground-state and first-excited-state transitions are shown in Fig. 2. The error bars represent the statistical errors from the

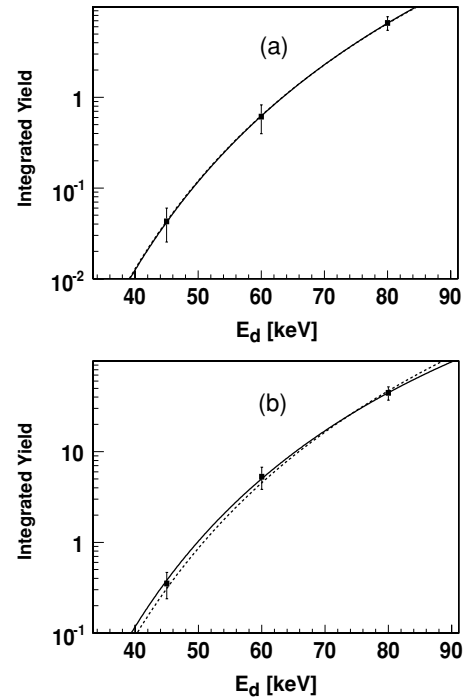


FIG. 2. Measured energy-integrated yields for (a) ${}^7\text{Li}(d,n_0){}^8\text{Be}$ and (b) ${}^7\text{Li}(d,n_1){}^8\text{Be}$ plotted at the incident beam energy. The error bars include statistical and systematic uncertainties. The solid lines were obtained by assuming an S factor that varies linearly with deuteron energy; the dashed lines were obtained by assuming a constant S factor (zero slope).

raw yields and the systematic errors from fitting the response functions to the spectra. The two curves shown in each plot are the best fits to the experimental results under the assumption that the S factor is constant with energy (dotted line) or varies linearly (nonzero slope, solid line). The numerical results and the corresponding χ^2 values are given in Table II. As seen in Fig. 2 and from the χ^2 values in Table II, the linear fit with a negative slope is much better than the constant fit for the n_1 transition, but the addition of a nonzero slope in the n_0 case changes little. Therefore, for the n_0 case, a zero slope is the best fit for the data.

For the n_1 transitions, this negative slope makes a significant difference in the $S(0)$ value, as is shown in Fig. 3. The $S(0)$ value for the linear $S(E)$ is a factor of 1.6 greater than that for a constant $S(E)$ for the n_1 neutron group.

Electron screening effects, which are discussed in detail in [10], are expected to give the S factor a negative slope at very low energies. For ${}^7\text{Li} + d$, this is anticipated to

TABLE II. Numerical values for the constant and linear $S(E)$ fits to the experimental yields.

State	$S(E) = S_0 + S_1 E$ [keV b]	χ^2
n_0	$S(E) = 430(\pm 120)$	0.032
	$S(E) = 400(\pm 200) + 0.62(\pm 3.3)E$	0.030
n_1	$S(E) = 3100(\pm 750)$	2.2
	$S(E) = 5000(\pm 1500) - 37(\pm 21)E$	0.62

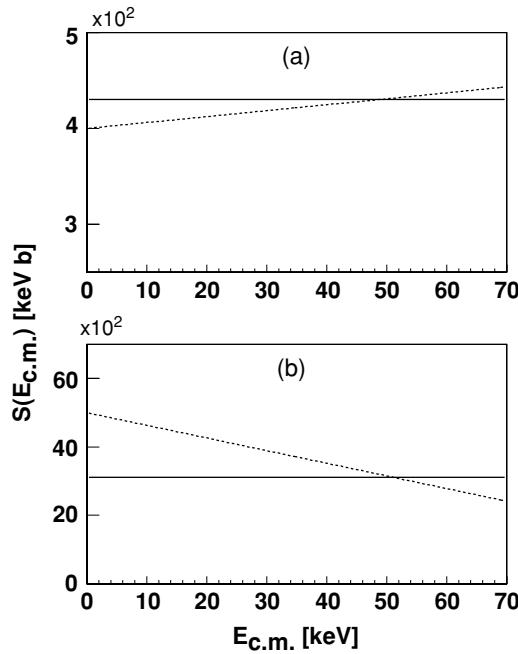


FIG. 3. Comparison of the constant $S(E)$ result (solid line) and the linear, nonzero-slope $S(E)$ result (dotted line) for the (a) n_0 and (b) n_1 groups. In the n_1 case, the slope of the S factor makes a significant difference in the value of $S(0)$.

only significantly influence the results for incoming deuteron beam energies of $E_d < 50$ keV. In the present experiment, the incident deuterons slow from the beam energy to zero within the target, but because the cross section decreases exponentially with decreasing deuteron energy, most of the yield will occur for the initial higher energies in the target. For a deuteron beam with $E_d = 45$ keV, the energy at which 50% of the yield is produced is $E_{50} = 43$ keV, and that at which 90% of the yield is produced is $E_{90} = 37$ keV. Using the formalism of [10], electron screening would be expected to produce an average relative slope $S_1/S_0 = -0.006 \text{ keV}^{-1}$ for 45-keV incident deuterons on ${}^7\text{Li}$. We conclude that the negative relative slope of the (d, n_1) channel ($S_1/S_0 = -0.007 \pm 0.005 \text{ keV}^{-1}$) could be attributed to electron screening effects. Although the relative slope for the (d, n_0) channel is consistent with zero ($S_1/S_0 = 0.002 \pm 0.008 \text{ keV}^{-1}$), the uncertainty also allows for a slope compatible with screening effects.

Figure 4 shows the S -factor results of the present measurement along with previous results for ${}^7\text{Li}(d, n){}^8\text{Be}$. The solid line is the linear $S(E)$ result obtained from the analysis discussed here. The S factor for $n_0 + n_1$ is $S(E) = 5400(\pm 1500) - 37(\pm 21)E \text{ keV b}$. The data points of Ref. [3,4] and the line representing the assumptions of Ref. [1] are for all three neutron groups. Therefore, the present measurement can only act as a lower limit on these measurements. However, the small slope of the present result is in reasonable agreement with the zero-slope assumption of Ref. [1]. Boyd *et al.* [1] examined cross-section data measured by Ref. [2] and found that values obtained for $S(E)$ from those data were fairly constant from 1.6 to 2.0 MeV. They then assumed this constant value for the S factor and extrapolated it down to

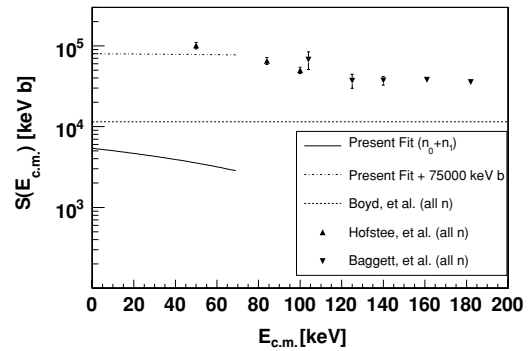


FIG. 4. Results of the present measurement (solid line) along with the previous data of Refs. [1,3], and [4]. The line assumed by Ref. [1] is based on data from Ref. [2]. The points for Ref. [4] were computed by assuming their differential cross-section data at 90° were isotropic, multiplying them by 4π to get the total cross section, and finally using the total cross section to deduce the S factor. It should be noted that the data for Refs. [1,3], and [4] include all neutron groups whereas the present result is for the n_0 and n_1 groups only. The dot-dashed line is the present result + $75,000 \text{ keV b}$, resulting from the best fit of a line with slope equal to the present slope of -37 b to the two lower energy points of Ref. [3].

zero energy [1]. To compare the slope of the present data with that of Ref. [3], their data points at $E_{c.m.} = 50$ and 83.5 keV were fitted to a line with slope equal to our slope of -37 b . The best fit resulted in a line equal to our line plus $75,000 \text{ keV b}$, or $80000 - 37E \text{ keV b}$. This line is shown in Fig. 4 as the dot-dashed line and indicates that the slope of the S factor at higher energies, as seen in the Hofstee *et al.* data, appears to be more negative than the slope of the present result. Note, however, that the present result does not include the n_2 neutron group.

Figure 5 shows the corresponding comparison of the total cross sections. The points representing the present

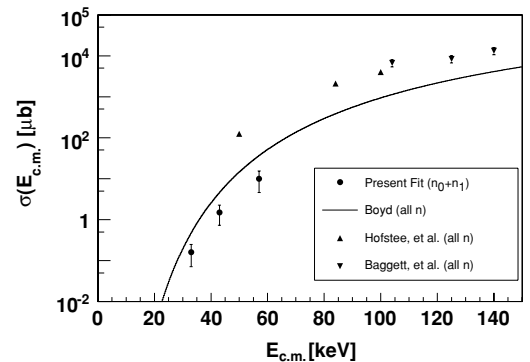


FIG. 5. Results of the present measurement (circular points) along with the previous data of Refs. [1,3] and [4]. The points for Ref. [4] were computed by assuming their differential cross-section data at 90° were isotropic and then multiplying them by 4π to get the total cross section. The line representing Ref. [1] was obtained by using the S -factor result they presented to compute the cross section. It should be noted that the data for Refs. [1,3] and [4] include all neutron groups whereas the present result is for the n_0 and n_1 groups only.

TABLE III. Numerical values for the absolute cross section for n_0 and n_1 as computed from the S factors $S(E) = 430(\pm 120)$ keV b and $S(E) = 5000(\pm 1500) - 37(\pm 21)E$ keV b, respectively.

$E_{\text{c.m.,eff}}$ [keV]	$\sigma_{\text{Total}}(E_{\text{c.m.,eff}})[\mu\text{b}]$	
	n_0	n_1
33	0.017 ± 0.0047	0.15 ± 0.066
43	0.17 ± 0.047	1.3 ± 0.67
57	1.3 ± 0.39	9.1 ± 6.0

measurements are plotted at the effective c.m. energy, that is, the energy at which half the yield is deposited in the target, and are the results for $n_0 + n_1$; these results are given in Table III. The present work lies below the (d,n) cross section calculated from the S factor given by Ref. [1], which is to be expected owing to the absence of the n_2 group in the present results. Hofstee *et al.* [3] measured the branching ratio of the ${}^7\text{Li}(d,n){}^8\text{Be} \rightarrow 2\alpha$ yields with respect to the yield of the ${}^6\text{Li}(d,p_0 + p_1)$ reaction and noted that contributions from ${}^6\text{Li}$ reactions complicated the spectra [3].

V. CONCLUSION

These measurements have determined the absolute astrophysical S factor and cross section for the ${}^7\text{Li}(d,n_0){}^8\text{Be}$ and ${}^7\text{Li}(d,n_1){}^8\text{Be}$ reactions at c.m. energies below 70 keV. The slope of the S factor is consistent with zero in the n_0 case but slightly negative in the n_1 case. The $S(E)$ for the ${}^7\text{Li}(d,n_0){}^8\text{Be}$ reaction was found to be $S(E) = 430(\pm 120)$ keV b, and that for the ${}^7\text{Li}(d,n_1){}^8\text{Be}$ reaction was found to be $S(E) = 5000(\pm 1500) - 37(\pm 21)E$ keV b. The total S factor for the ${}^7\text{Li}(d,n_0 + n_1){}^8\text{Be}$ reaction is $S(E) = 5400(\pm 1500) - 37(\pm 21)E$ keV b, where E is the c.m. energy in keV for all three results. The negative value of the slope is consistent with the value expected from an estimate of the effects resulting from electron screening. We therefore recommend that this slope should not be included in determining the S factor at zero energy.

ACKNOWLEDGMENTS

This work was partially supported by the U. S. Department of Energy under Grant N.S. DE-FG02-97ER41046, DE-FG02-97ER41033, and DE-FG02-97ER41042.

- [1] R. N. Boyd, C. A. Mitchell, and B. S. Meyer, Phys. Rev. C **47**, 2369 (1993).
 [2] J. C. Slattery, R. A. Chapman, and T. W. Bonner, Phys. Rev. **108**, 809 (1957).
 [3] M. A. Hofstee, A. K. Pallone, F. E. Cecil, J. A. McNeil, and C. S. Galovich, Nucl. Phys. **A688**, 527c (2001).
 [4] L. M. Baggett and S. J. Bame, Phys. Rev. **85**, 434 (1952).
 [5] R. M. Prior, *et al.*, Phys. Rev. C **70**, 055801 (2004).
 [6] G. Dietz and H. Klein, *NRESP4 and NEFF4 Monte Carlo Codes for the Calculation of Neutron Response Functions*

and Detection Efficiencies for NE 213 Scintillation Detectors (Physikalisch-Technische Bundesanstalt, Bundesallee 100, W-3300 Braunschweig, 1982).

- [7] D. E. Gonzalez Trotter, Ph.D. thesis, Duke University, 1997.
 [8] F. Salinas Meneses, Ph.D. thesis, Duke University, 1998.
 [9] H. H. Anderson and J. F. Ziegler, *Hydrogen Stopping Powers and Ranges in All Elements* (Pergamon, London, 1977).
 [10] M. Lattuada, R. G. Pizzone, S. Typel, P. Figuera, D. Miljanic, A. Musumarra, M. G. Pellegritti, C. Rolfs, C. Spitaleri, and H. H. Wolter, Astron. J. **562**, 1076 (2001).